Applied Catalysis B: Environmental 300 (2022) 120721

Contents lists available at ScienceDirect

Applied Catalysis B: Environmental

journal homepage: www.elsevier.com/locate/apcatb

Glaser coupling- and Sonogashira coupling-control over Cu_xO nanoparticles/carbon nanotube by switching visible-light off and on

Yiwei Zhou, Jian Zhao *

Tianjin Key Laboratory of Organic Solar Cells and Photochemical Conversion, School of Chemistry and Chemical Engineering, Tianjin University of Technology, Tianjin 300384, PR China

ARTICLE INFO

Keywords:
Visible-light
Sonogashira coupling
Glaser coupling
CuxO nanoparticles
Carbon nanotubes

ABSTRACT

Utilizing Cu_xO nanoparticles supported on carbon nanotube as catalyst, visible-light could efficiently transform Glaser homo-coupling into Sonogashira cross-coupling. The isolated Sonogashira product yield is up to 0.58 mmol (sel. 97%) under visible-light irradiation while the Glaser product achieves 0.45 mmol (sel. 92%) in the dark for phenylacetylene and iodobenzene. We also discover that the active species under light irradiation is different from that in the dark. The visible light-driven adsorption of aromatic iodides on Cu_xO nanoparticles and light-excited copper(I) phenylacetylide intermediates together enables the high selectivity of Sonogashira product. The synergistic effect between Cu(II) and Cu(I) acetylide dimer complex enhances the Glaser product yield in the dark.

1. Introduction

Carbon-carbon bond formation is critically important in organic chemistry [1]. As known, there are several types of C-C coupling reactions [2–6]. The Sonogashira and Glaser coupling are such popular ones.

The Sonogashira cross-coupling of terminal alkynes with aryl and vinyl halides was first systematically studied with catalytic amounts of $Pd(PPh_3)_2$ and CuI in 1975 [7]. Over the past 45 years, noble metal catalysts such as palladium- and gold-based systems have been developed for this C-C cross-coupling reaction [8–11]. Due to the low abundance and high cost of noble metals, transition metals such as iron, copper, nickel, etc. attract more and more attentions [12–14]. It has been reported that copper nanomaterials could catalyze Sonogashira coupling by adding ligands at high temperatures [12]. There are few reports on light-driven Sonogashira coupling over copper-based nanomaterials except two works reported in 2019 and 2020 [15,16]. However, the reduction of catalytic sites CuO was accompanied by the oxidation of Ti (III) to Ti (IV), with a yield of only ~0.09 mmol for Sonogashira product [15] or CO_2 was necessary to achieve high selectivity over Cu_2O [16].

Glaser homo-coupling is the self-coupling of alkynes, first discovered in 1869 [17]. Palladium- and Cu-based salts were generally used as catalyst, in the presence of ligands [18,19]. Various copper-based systems have been studied although the exact mechanism is not fully understood [20,21]. Therefore, it is highly important to design efficient copper-based nanocatalysts and differentiate the active species between Glaser homo-coupling and Sonogashira cross-coupling reactions.

Selectivity is also significantly important in organic synthesis. Up to date, there is no report on efficient heterogeneous catalytic systems for controlling Sonogahsira and Glaser coupling with high yield and selectivity. Light seems to be a promising star for selectivity control under mild conditions [22–26]. Therefore, it is desirable to develop new photocatalytic systems to efficiently control Sonogashira coupling and Glaser coupling with light irradiation. Switching visible-light off and on, here, we give a first report that Glaser homo-coupling and Sonogashira cross-coupling could be simply switched over carbon nanotubes-supported Cu_xO nanoparticles (Cu_xO/CNTs).

2. Experimental

2.1. Materials preparation

2.1.1. Materials and chemicals

Carbon nanotubes (Multi-walled, 10–20 nm (diam.), 5–15 μm (length)), carbon nanofibers (> 70%, 200–600 nm (outsider diameter), 5–50 μm (length)), copper (II) chloride dihydrate (98%), glucose (92%), sodium hydroxide (97%), potassium carbonate (99%), DMF (HPLC),

* Corresponding author.
E-mail addresses: zjtjbd@hotmail.com, zjtjbd@email.tjut.edu.cn (J. Zhao).

https://doi.org/10.1016/j.apcatb.2021.120721
Received 19 May 2021; Received in revised form 24 August 2021; Accepted 12 September 2021
Available online 16 September 2021

iodobenzene (99%), phenylacetylene (98%), copper(I) phenylacetylide (97%), triethylamine (99.5%), sodium carbonate (99%), potassium bicarbonate (99.7+%), cesium carbonate (99.9%), ethanol (95%), acetonitrile (99.5%), tetrahydrofuran (99%), ultrapure water (18.2 MΩ cm). All chemicals were used as received without further purification.

2.1.2. Preparation of CNTs supported Cu_xO NPs

The supported Cu_xO nanoparticles (NPs) were prepared by an impregnation method modified from literatures [27]. In a typical preparation, 1 g carbon nanotubes (CNTs) were introduced into a sealed vial bottle containing 10 mL aqueous solution of $CuCl_2$. After stirring at 90 °C for 1 h, NaOH and glucose were added respectively into the mixture solution. The molar ratio of NaOH/Cu was 4:1 and glucose/Cu was 4:1. The mixed solution were kept stirring at 90 °C for another 1 h. The Cu_xO/CNTs products were obtained by centrifuging and sufficiently washed three times with ultrapure water and finally dried at 110 °C overnight. The total amount of Cu in the prepared samples was determined by inductively coupled plasma atomic emission spectrometry (ICP). 2.6%Cu_xO/CNTs was used as typical catalyst if not specified. TiO_2(B) nanofibers were prepared through calcination of hydrogen titanate ($H_2Ti_3O_7$) fibers at 450 °C for 3 h while the synthesis of $H_2Ti_3O_7$ nanofibers was according to our previous works [23,28]. Cu(II)O/CNTs was prepared with the same procedure in the absence of glucose.

2.2. Characterization

X-ray diffraction (XRD) patterns of the samples were recorded on a Rigaku UItima IV diffractometer using Cu Kα radiation (λ = 1.5418 Å). The absorption spectra of the samples were determined using a UV-2600 spectrophotometer (Shimadzu). The investigation on the morphology and size of the catalysts was carried out on Talos F200 X with an accelerating voltage of 200 kV in scanning-transmission modes (STEM), using a High-Angle Annular Dark Field detector (HAADF). BET was tested on micromeritics ASAP 2020 PLUS HD88 to obtain the information of specific surface area of the samples. To investigate the Cu ionic states and Cu(I)/Cu(II) composition, X-ray photoelectron spectroscopy (XPS) measurements were performed (Thermo Scientific Escalab 250Xi) and the standard binding energy of C 1s is at 284.8 eV.

2.3. Photo/thermal catalytic reaction

100 mg Cu_xO/CNTs, 1.0 mmol alkyne, 1.5 mmol iodobenzene and 1.5 mmol potassium carbonate was added to 25 mL glass tube connected to a condenser tube and a balloon filled with H_2/Ar (5 vol%). The reaction mixture was stirred and irradiated with a Halogen lamp (0.75 W/cm^2 if not specified). The temperature of the reaction mixture was carefully controlled with cooling system and thermometer was used to monitor the environmental temperature (40, 60, 80, 100, 120 °C respectively corresponds to 60, 80, 100, 120, 130 °C solvent temperature). The corresponding dark reaction was conducted in oil bath with temperature set to 80 °C~140 °C. After reaction, 0.5 mL aliquots were collected and then filtered through a Millipore filter (pore size 0.45 μm) to remove the catalyst for GC and GC-MS analysis. The reaction mixture was purified by column chromatography on silica gel using different ratios of petroleum ether and ethyl acetate as eluent. The isolated products were analyzed with ^1H and ^{13}C NMR (Bruker-400 MHz).

The experiment details for Fig. 4. for (1) and (2), 1.0 mmol copper phenylacetylide was used instead of 1.0 mmol phenylacetylene without the addition of Cu_xO/CNTs. To keep the same amount of Cu with (1) and (2), 0.9 mmol copper phenylacetylide and 232.6 mg Cu_xO/CNTs was added for (3). Other experiment conditions are the same as above.

3. Results and discussion

3.1. The characterization of Cu_xO NPs/CNTs

The size distribution of Cu_xO nanoparticles is from 1 nm to 3 nm with average sizes 1.96 ± 0.75 nm, as shown in Fig. 1a. The presence of both Cu(I) and Cu(II) in Cu_xO nanoparticles is proved by XPS analysis (Fig. S1). The existence state of Cu(II) species is probably amorphous since only Cu_2O crystallite as Cu(I) species is observed in XRD pattern in Fig. 1b, where the diffraction peak at 36.4°, 42.3°, 61.3° and 73.5° are corresponding to Cu_2O (111), (200), (220) and (311), respectively (JCPDS#05-0667).

3.2. Photo/thermal catalytic Sonogashira and Glaser coupling

As shown in Fig. 2a and b, prolonging the reaction time, Sonogashira coupling increase under light irradiation while Glaser coupling increase in the absence of light. Only negligible Glaser product is observed under light irradiation. After removing the catalyst, the product yields stop increasing which indicates that the reaction is driven by heterogeneous Cu_xO/CNTs catalyst. Here, DMF and K_2CO_3 were chose according to the activity data from various types of solvent and base (Table S1). The reaction was conducted under H_2/Ar atmosphere since oxygen indeed shows negative effects on the catalytic activity of Cu_xO/CNTs, where the yield of Sonogashira product decrease from 0.60 mmol to 0.51 mmol and 0.48 mmol for H_2/Ar, air, O_2 atmosphere respectively. Without light irradiation, increasing the solvent temperature to 140 °C cannot achieve high yield and selectivity of Sonogashira product (Fig. S2).

Chopping experiments show that the Sonogashira coupling increases with the light on and decreases with light off (Fig. 3a). All these results demonstrate that visible-light irradiation is essential to switch Glaser coupling to Sonogashira coupling. A linear relationship between product yield and light intensity is also observed when $0.29\ W/cm^2 \leq I_{light} \leq 0.75\ W/cm^2$ (Fig. 3b), consistent with other photocatalysts systems [29,30]. Utilizing CNTs as catalyst, no products were observed. Thus, Cu_xO nanoparticles are the active cites for the reaction. Due to the strong light absorption of CNTs in the visible-light range (Fig. 3c-i), Cu_xO/TiO_2(B) nanofiber was prepared to determine the light absorption of Cu_xO nanoparticle (Fig. 3c-ii). Kept at same light intensity, the effect of light wavelength on the activity is investigated. From the action spectrum in Fig. 3c, wide light range obviously suppresses the self-coupling of phenylacetylene. The yield of Glaser product obviously increases from cut-400 nm to cut-470 nm and cut-630 nm, matched with the absorption spectra of Cu_xO nanoparticles. The dramatic increase is observed with light wavelength between cut-400 nm and cut-470 nm. This demonstrates that shorter wavelength 400–470 nm contributes more to inhibit Glaser coupling and promote the formation of Sonogashira product.

The supports effect on the photocatalytic activity of Cu_xO nanoparticles is also investigated (Table S2). With similar XRD, XPS and size distribution (Figs. S4–S6), Cu_xO nanoparticles on TiO_2(B) nanofibers exhibit much lower photocatalytic activity (0.16 mmol) than that on CNTs (0.60 mmol, 123 m^2/g), which probably caused by its low specific surface area (37 m^2/g). However, with a lower specific surface area compared to TiO_2(B) nanofiber, carbon nanofiber (12 m^2/g)-supported Cu_xO nanoparticles achieve a yield of 0.25 mmol. The low activity of Cu_xO on TiO_2(B) is probably due to low adsorption capability of TiO_2(B) for iodobenzene (0.1 mmol, 1 h), compared with CNTs (0.3 mmol, 1 h).

3.3. Mechanism investigation

Copper(I) phenylacetylide acts as active intermediate for photocatalytic reactions have been reported [31–33]. In our system, the action spectrum in Fig. 3c matches well with light absorption of copper(I) phenylacetylide (Fig. S7). We also confirm the formation of copper(I) phenylacetylide via UV-Vis spectra over phenylacetylene-adsorbed

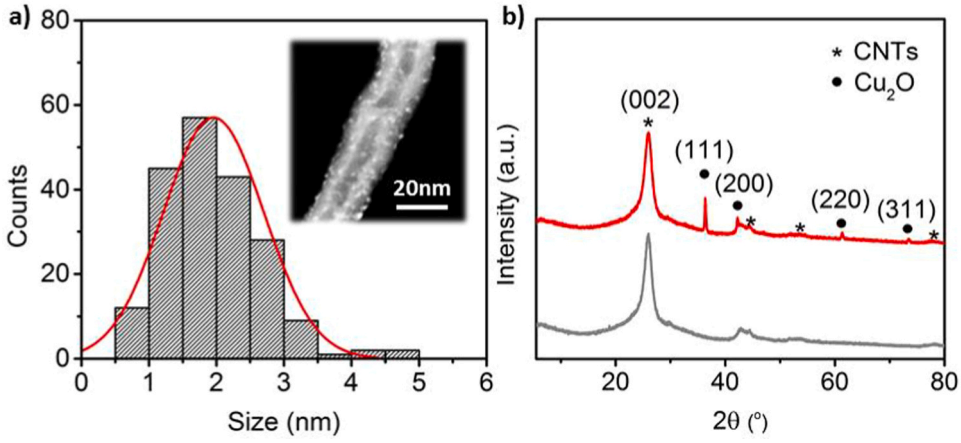

Fig. 1. Size distribution with dark field image inset (a) and XRD pattern (b) of Cu_xO nanoparticles on CNTs.

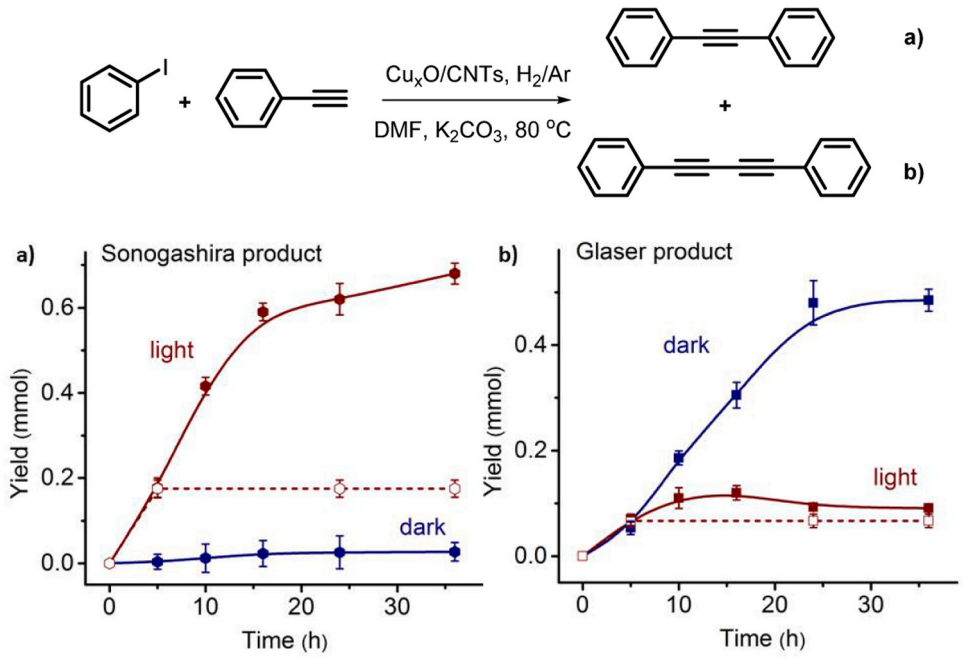

Fig. 2. The time-yield curves of Sonogashira and Glaser coupling under light irradiation and in the dark. The dash line is the yield change after removing the catalyst. Only 0.6% biphenyl side product is detected under light irradiation. GC-MS spectra of the products are provided in Fig. S3. The NMR data are also given in SI. (1.0 mmol phenylacetylene, 1.5 mmol iodobenzene, 1.5 mmol K_2CO_3, 2 mL DMF, 100 mg Cu_xO/CNTs, 0.75 W/cm^2, 80 °C, H_2/Ar).

sample (Fig. S8). Thus, the active species under light irradiation is further investigated by employing copper (I) phenylacetylide as reactant. As given in Fig. 4-(1), similar Sonogashira product yield (0.58 mmol) is observed for copper(I) phenylacetylide as that for phenylacetylene and Cu_xO/CNTs (0.60 mmol) under the same experiment conditions. However, the selectivity for Sonogashira coupling decreased to $< 70\%$ since 0.12 mmol Glaser product was detected. Then, we believe that Cu_xO play an important role in the activation of iodobenzene, in turn promoting the Sonogashira product selectivity. When Cu_xO/CNTs was added, the Glaser product decreased to < 0.04 mmol (Fig. 4-(3)). This proves that light-excited Cu_xO nanoparticle could inhibit the Glaser coupling pathway by activating iodobenzene, compared with light-excited copper(I) phenylacetylide counterpart. Phenylacetylene was also added to the mixture for Fig. 4 (2) and (3) (Fig. S9) and the Glaser product under light irradiation increased from 0.15 mmol to 0.46 mmol. This demonstrates that copper(I) phenylacetylide could catalyze phenylacetylene home-coupling in the presence of light, in agreement with the reported work [16]. The addition of Cu_xO/CNTs could dramatically reduce the Glaser product yield from 0.46 mmol to 0.25 mmol, which further proves the critical role of light activating iodobenzene on Cu_xO for the formation of Sonogashira product. Therefore, various methods were utilized to further investigate the activation or chemiadsorption of iodobenzene on Cu_xO/CNTs.

As shown in Fig. 5, the two peaks of I $3d_{5/2}$ and I $3d_{3/2}$ at 619.5 eV and 630.9 eV in XPS spectra for iodobenzene adsorbed on Cu_xO/CNTs after light irradiation (ii) are more intense than that in the dark (i), which is the characteristic of chemiadsorbed iodine [34], while the relative ratio of Cu(I)/Cu(II) keeps unchanged. To exclude the influence of CNTs, the adsorption experiment was further conducted over Cu_xO prepared in the absence of CNTs support. The XRD pattern and XPS spectra of Cu_xO before and after adsorption remain the same (Figs. S11-S12). Compared with the results in the dark, there is an obvious color change and appearance of absorption peak at 600–800 nm for the adsorbed sample irradiating with light after 1 h (Fig. 6). Analyzed from the corresponding FT-IR spectra, the C-I stretching mode $\nu_{C\text{-}I}$ at 1059 cm^{-1} shifts to 1077 cm^{-1}, the ring breathing mode at

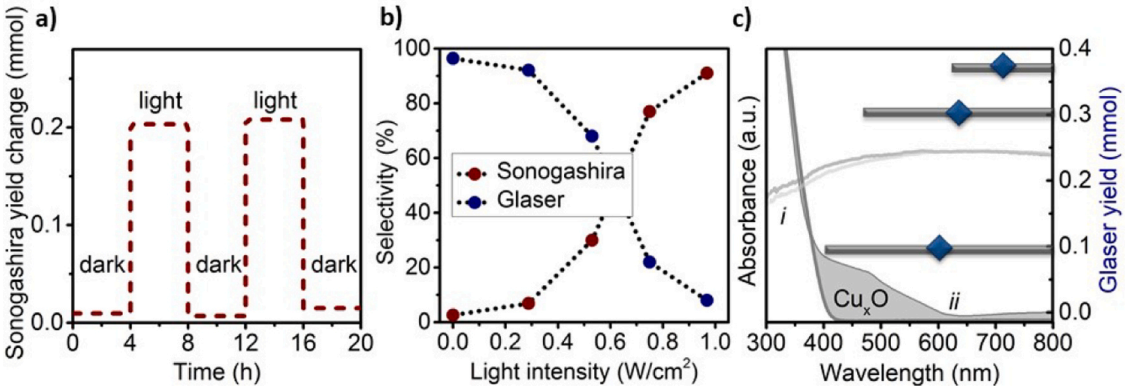

Fig. 3. The influence of light on the products yield and selectivity (a) chopping experiments, obtained from origin data via subtraction (b) light intensity I_{light} and (c) light wavelength. i-CNTs and Cu_xO/CNTs, ii-TiO_2(B) and Cu_xO/TiO_2(B) nanofibers. The square represents Glaser yield under light irradiation with collective wavelength (horizontal column) for cut-400 nm, cut-470 nm and cut-630 nm. (1.0 mmol phenylacetylene, 1.5 mmol iodobenzene, 1.5 mmol K_2CO_3, 2 mL DMF, 100 mg Cu_xO/CNTs, 0.75 W/cm^2, 80 °C, H_2/Ar, 24 h).

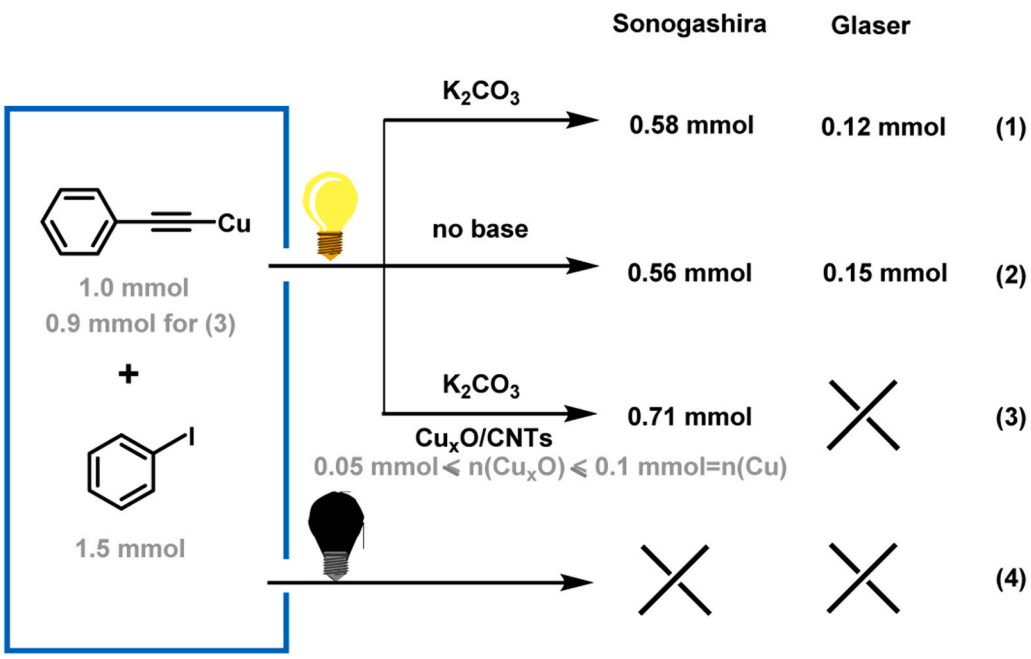

Fig. 4. Mechanistic studies on the active species responsible for the activation of phenylacetylene and iodobenzene under light irradiation (1.5 mmol K_2CO_3, 2 mL DMF, 0.75 W/cm^2, 80 °C, H_2/Ar, 24 h).

998 cm^{-1} shifts to 989 cm^{-1}, the two C-H out-of-plane bending mode $\gamma_{C\text{-}H}$ at 903 cm^{-1} and 834 cm^{-1} respectively shift to 928 cm^{-1} and 825 cm^{-1}, while the peak at 683 cm^{-1} ascribed to the nonplanar twist mode χC-C-C shifts to 693 cm^{-1} [35,36]. This could conclude that special bonding is formed between iodobenzene and the surface of Cu_xO under visible-light irradiation. In addition, different from radical approach in homogenous Cu systems [1,37], the activation of iodobenzene on Cu_xO will form active intermediates instead of radicals since there is no decrease of product yield when (1/3, 2/3, 4/3 equiv) TEMPO was added as radical inhibitor.

Moreover, similar amount of Sonogashira product was detected in the presence and absence of base, (1) and (2) in Fig. 4. Therefore, the base is mainly responsible for the formation of active species copper (I) phenylacetylide and has no influence on the following reaction steps.

As shown in Figs. 4-(4) and 7-(1), copper(I) phenylacetylide is not active for the formation of Glaser product in the dark since negligible product was detected. In addition, small amount of precipitate phase in filtrate was observed for the reaction in the dark and analyzed to be copper(I) phenylacetylide (Fig. S13), which further confirms that it does not take part in the Glaser coupling in the dark. Although the mechanism of Glaser coupling is complicated and not fully understood, copper(II) acetylide dimeric complex is accepted [38,39]. We also confirmed that Cu(II) salt itself could catalyze Glaser coupling reaction in the dark (Fig. 7-(2)). The presence of copper(I) phenylacetylide and Cu(II) achieved (Fig. 7-(3)) higher Glaser product yield than Cu(II) alone. In our system, the synergistic effect of Cu(II) and Cu(I) for the activation of phenylacetylene in the dark was further illustrated by the dramatically decreased Glaser product utilizing supported Cu(II)O instead of Cu_xO, from 0.48 mmol to 0.34 mmol (Fig. 7-(4) and (5)). The XRD and XPS analysis of supported Cu(II)O nanoparticles are provided in Figs. S14 and S15. The Cu(II) and Cu(I) dimeric complex is also verified as active species for alkynes homo-coupling reaction with $CuCl_x(TMEDA)_{3-x}$ catalyst [40]. Thus, we proposed a scheme for the synergistic effect of Cu (II) and Cu(I) in the dimer complex, resulting in the high selectivity of Glaser product (Scheme S1).

The Sonogashira reaction was inhibited when $K_2S_2O_8$ were employed

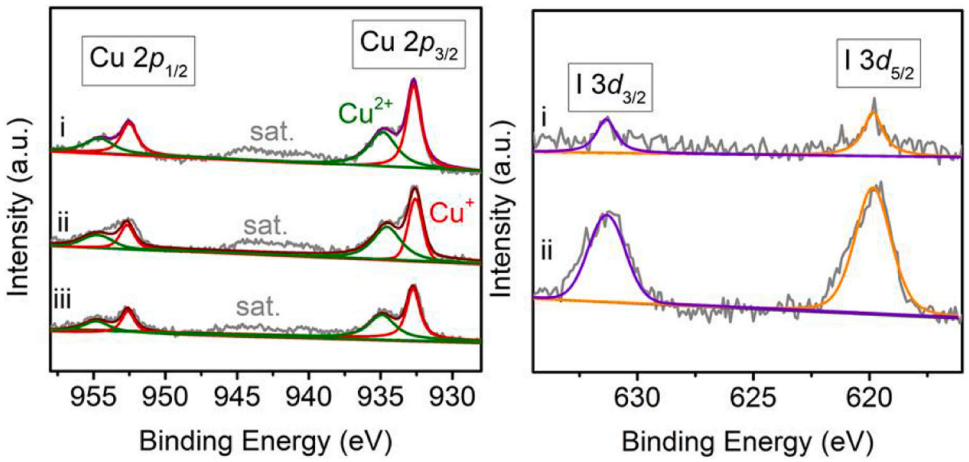

Fig. 5. XPS analysis of Cu 2*p* and I 3*d*. (i) after adsorption of iodobenzene in the dark (80 °C), (ii) after adsorption of iodobenzene under light irradiation (0.75 W/cm^2, 80 °C), (iii) pure Cu_xO/CNTs. C1s is provided in Fig. S10.

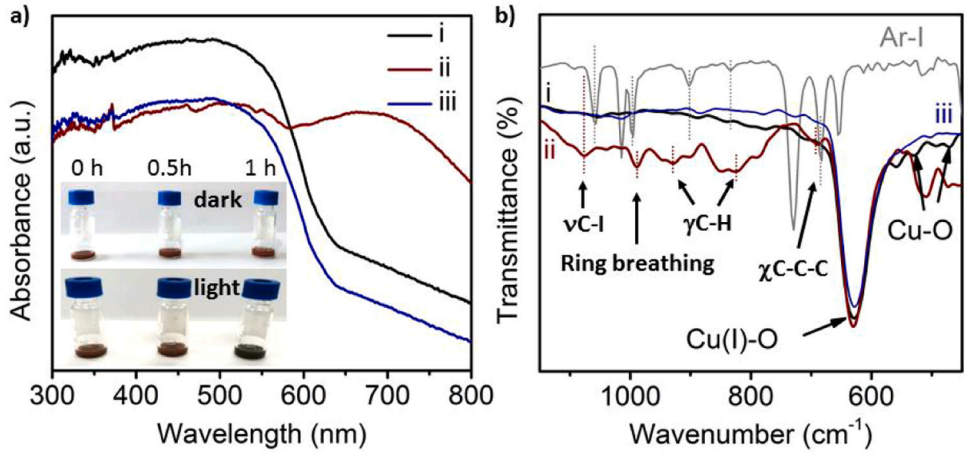

Fig. 6. UV-Vis and FT-IR spectra of (i) Cu_xO, after iodobenzene adsorption (ii) under light and (iii) in the dark for 1 h at 80 °C. The inset photo is taken before and after adsorption for 0.5 h and 1 h, in the absence and presence of light.

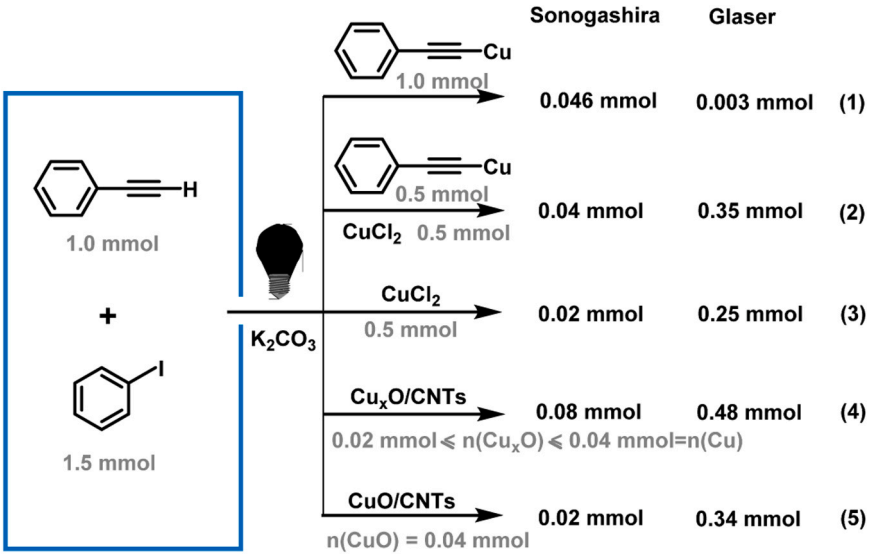

Fig. 7. Mechanistic studies on the synergistic effect of Cu(II) and Cu(I) for the activation of phenylacetylene in the dark, resulting in high selectivity of the Glaser product. (1.5 mmol K_2CO_3, 2 mL DMF, 80 °C, H_2/Ar, 24 h).

as quenchers for electrons. This indicates that photogenerated electrons involves in the reaction for the cross-coupling, probably inhibit the formation of long-lived Cu(I) phenylacetylide under light irradiation. The lifetime of Cu(I) phenylacetylide powder and that dispersed in DMF was tested to be 0.2 μs and 0.25 μs (Fig. S16), respectively. All these results confirm that light is essential to excite copper(I) phenylacetylide for driving Sonogashira coupling.

3.4. Proposed mechanism

Based on above experiments results, we proposed the photocatalytic reaction mechanism in Scheme 1. In step 1, copper(I) phenylacetylide and Cu(II)-Cu(I) dimeric acetylide could be formed in the presence of base. In the presence of light (left), the following step is photoexcitation of Cu(I) phenylacetylide by visible-light irradiation, resulting in the formation of electron-deficient acetylene moiety via ligand to metal charge transfer, favorable for the following attack of iodobenzene. Simultaneously, iodobenzene is photo-assisted activated on the surface of supported Cu_xO nanoparticle via the C-I bond and benzene ring, as illustrated in Fig. 6. The final step is the addition of excited Cu(I) phenylacetylide and active intermediates of iodobenzene, forming final Sonogashira product and HI. The formation of HI under light irradiation was proved by chemical reactions and no HI was observed in the dark (Fig. S17). In the dark (right), Cu(II)-Cu(I)-acetylide dimeric complex react with another phenylacetylene with the assistance of base, followed by the formation of Glaser product.

The apparent activation energies for the Sonogashira and Glaser reactions over Cu_xO/CNTs are determined by using the Arrhenius equation and the kinetics data of the reactions conducted under various temperatures. The apparent activation energy for the Sonogashira reaction under visible light irradiation is 56.4 kJ/mol, lower than that for the Glaser reaction in the dark, 76.3 kJ/mol (Fig. S18). This value (56.4 kJ/mol) is similar with the apparent activation energy for Sonoghashira reaction over Pd/SiC under light irradiation (~64.3 kJ/mol), whereas much lower than that for Sonogashira reaction in the dark (~72.3 kJ/mol) [41]. In our system, however, the apparent activation energies for the Sonogashira reaction in the dark and Glaser reaction under visible light are not compared since the corresponding yield of Sonogashira product and Glaser product is too low to make sure the accuracy of the results.

3.5. Various substrates

Various substituted substrates were also investigated under optimal reaction conditions (Table 1). The substituted iodobenzene with electron-donating groups at *para*-position (entry 2 and 3) show similar Sonogashira and Glaser product yields compared with non-substituted counterpart (entry 1), under light and in the dark, respectively. With strong electron-withdrawing group (entry 4), e.g. *p*-NO_2, it gives much higher Sonogashira product under light irradiation (the reaction time is reduced to 12 h). This further support the proposed mechanism since it is easy for the abstraction of I over Cu_xO, forming Sonogashira product and HI. Low yields of Glaser product in the dark for phenylacetylene with electron-donating groups at para-position (entry 5 and 6) were observed.

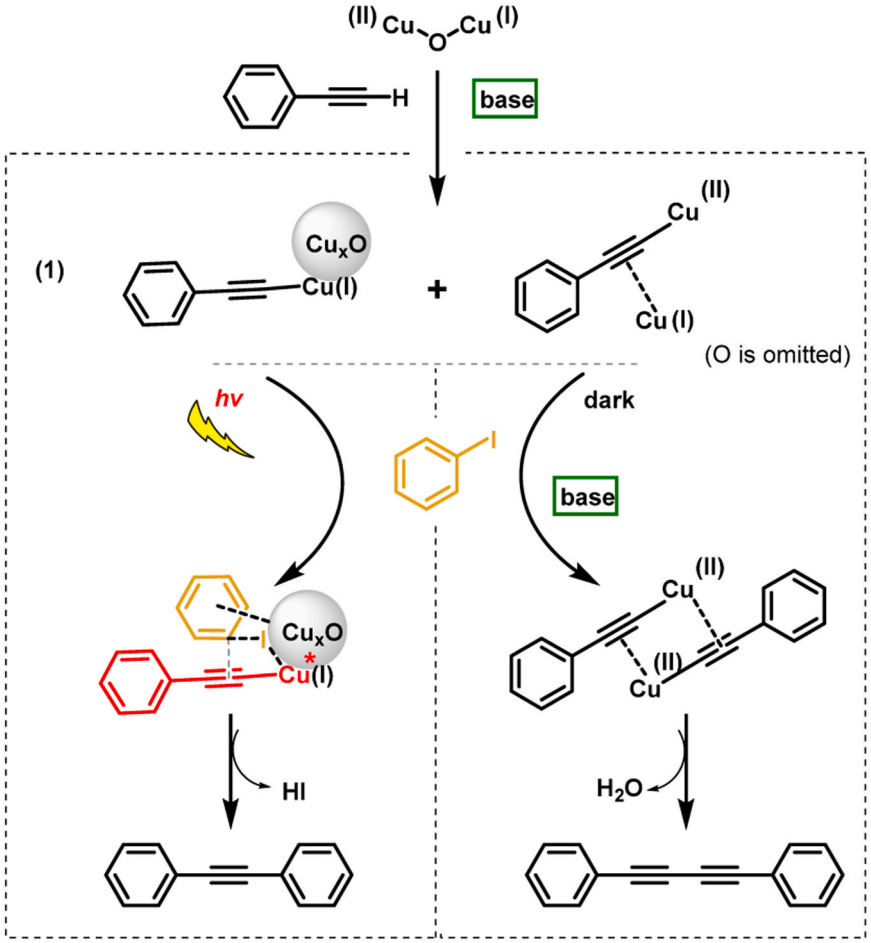

Scheme 1. The main reaction pathway for Sonogashira and Glaser coupling over Cu_xO/CNTs under light and in the dark, respectively. The proposed scheme for the synergistic effect of Cu(II) and Cu(I) on homo-coupling in the dark is provided in Scheme S1.

Table 1
The reaction of various substituted substrates under light and in the dark.[1]

Entry	Substrate 1	Substrate 2	Sonogashira yield (mmol)[2]		Glaser yield (mmol)[2]	
			Light	Dark	Light	Dark
1		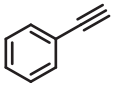	0.58	0.08	0.01	0.45
2	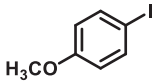	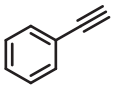	0.62	0.08	0.03	0.45
3	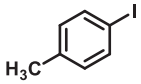	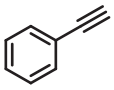	0.60	0.01	0.07	0.43
4[3]	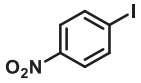	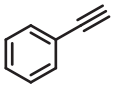	0.62	0.16	0.05	0.47
5		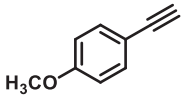	0.25	0.01	0.003	0.12
6		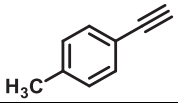	0.25	0.01	0.003	0.05

[1] Reaction conditions: 1.5 mmol substrate 1, 1.0 mmol substrate 2, 1.5 mmol K_2CO_3, 2 mL DMF, 100 mg Cu_xO/CNTs, 0.75 W/cm^2, 80 °C, H_2/Ar, 24 h.
[2] Isolated yield. ^{1}H NMR and ^{13}C NMR for the products are given in SI.
[3] The reaction time under light irradiation is only 12 h whereas in the dark is still 24 h.

3.6. Stability and reusability of Cu_xO/CNTs

The main Sonogashira product under light and Glaser product in the dark are maintained for the recycling experiments (Fig. 8). However, there is an obvious decrease for the activity. The recycled sample shows a decrease of Cu_xO content confirmed by ICP and a decrease of Cu(I) verified by XPS (Fig. S19). The influence of Cu_xO content could be excluded since the prepared 1.6 wt% Cu_xO/CNTs achieves similar activity with 2.6 wt% Cu_xO/CNTs (Table S3). Thus, the decrease of the activity is probably due to the loss of Cu(I), in agreement with our hypothesis that light-excited Cu(I) phenylacetylide is mainly responsible for Sonogashira product and the synergistic effect between Cu(I) and Cu (II) promotes the Glaser product in the dark. Reactivation of the recycled catalyst with glucose as a reducing agent at 90 °C for 1 h could increase the ratio of Cu(I)/Cu(II) (Fig. S20), resulting in the increase of Sonogashira product from 0.32 mmol to 0.48 mmol (24 h).

4. Conclusions

In summary, we report the first example of efficient Sonogashira and Glaser transformation tuned by visible-light over Cu_xO/CNTs. More importantly, we demonstrate that copper(I) phenylacetylide intermediate is the active species for Sonogashira coupling in the presence of visible light rather than that for Glaser coupling in the dark. The interaction between Cu_xO and iodobenzene under light irradiation could promote Sonogashira coupling. The simultaneously light-activated aromatic iodide on Cu_xO nanoparticles and light-excited copper phenylacetylide are essential to achieve high selectivity of Sonogashira product. The strategy reported here is expected to attract interesting for nanomaterial design and selectivity control in organic chemistry. This study may also give new insights into the fundamental mechanistic understanding, especially on copper-based heterogeneous systems for Sonogashira- and Glaser- type reactions.

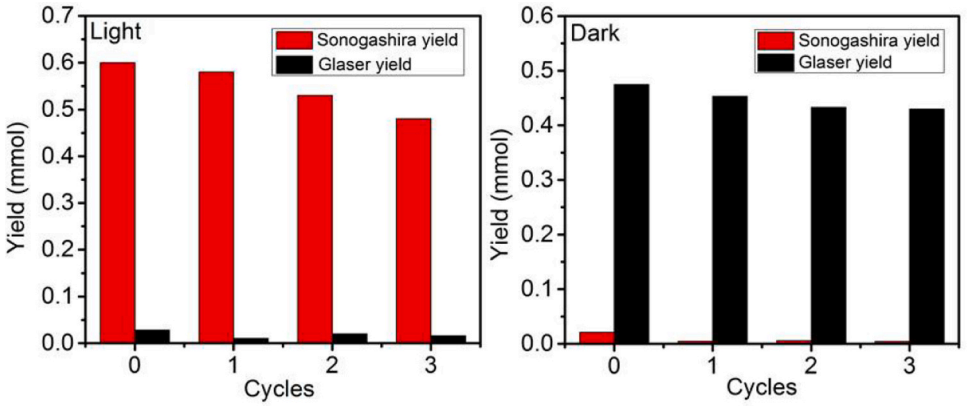

Fig. 8. The recycling experiments of Cu_xO/CNTs for the reaction between iodobenzene (1.5 mmol) and phenylacetylene (1.0 mmol) under light and in the dark. 1.5 mmol K_2CO_3, 2 mL DMF, 100 mg Cu_xO/CNTs, 0.75 W/cm^2, 80 °C, H_2/Ar, 24 h for fresh samples and 36 h for recycled samples.

CRediT authorship contribution statement

Yiwei Zhou: Investigation, Methodology, Data curation, Validation. **Jian Zhao**: Conceptualization, Supervision, Writing – original draft, Writing – review & editing.

Declaration of Competing Interest

There are no conflicts to declare.

Acknowledgements

Financial support of this work by the National Science Foundation of China (NSFC, 21703154) and the Natural Science Foundation of Tianjin (18JCYBJC43100) is gratefully acknowledged.

Appendix A. Supporting information

Supplementary data associated with this article can be found in the online version at doi:10.1016/j.apcatb.2021.120721.

References

[1] X.Y. Dong, Y.F. Zhang, C.L. Ma, Q.S. Gu, F.L. Wang, Z.L. Li, S.P. Jiang, X.Y. Liu, A general asymmetric copper-catalysed sonogashira c(sp(3))-c(sp) coupling, Nat. Chem. 11 (2019) 1158–1166.
[2] N. Miyaura, K. Yamada, A. Suzuki, A new stereospecific cross-coupling by the Palladium-catalyzed reaction of 1-alkenylboranes with 1-alkenyl or 1-alkynyl halies, Tetrahedron Lett. 36 (1979) 3437–3440.
[3] F. Ullmann, J. Bielecki, Synthesis in the biphenyl series, Eur. J. Inorg. Chem. 34 (1901) 2174–2185.
[4] T.H. Yasuo Hatanaka, Cross-coupling of organosilanes with organic halides mediated by Palladium catalyst and tris(diethylamino)sulfonium difluorotrimethylsilicate, J. Org. Chem. 53 (1988) 918–920.
[5] R.F. Heck, Arylation, methylation, and carboxyalkylation of olefins by group VIII metal derivatives, J. Am. Chem. Soc. 90 (1968) 5518–5526.
[6] K.F. Heck, J.P. Nolley Jr., Palladium-catalyzed vinylic hydrogen substitution reactions with aryl, benzyl, and styryl halides, J. Org. Chem. 37 (1972) 2320–2322.
[7] K. Sonogashira, Y. Tohda, N. Hagihara, A convenient synthesis of acetylenes: catalytic substitutions of acetylenic hydrogen with bromoalkenes, iodo arenes, and bromopyridines, Tetrahedron Lett. 50 (1975) 4467–4470.
[8] C. Gonzalez-Arellano, A. Abad, A. Corma, H. Garcia, M. Iglesias, F. Sanchez, Catalysis by gold(I) and gold(III): a parallelism between homo- and heterogeneous catalysts for copper-free Sonogashira cross-coupling reactions, Angew. Chem. Int. Ed. 46 (2007) 1536–1538.
[9] B. Wang, Y.Y. Wang, J.Z. Li, X.N. Guo, G.L. Bai, X.L. Tong, G.Q. Jin, X.Y. Guo, Photocatalytic Sonogashira reaction over silicon carbide supported Pd-Cu alloy nanoparticles under visible light irradiation, Catal. Sci. Technol. 8 (2018) 3357–3362.
[10] K.C. Dissanayake, P.O. Ebukuyo, Y.J. Dhahir, K. Wheeler, H.S. He, A BODIPY-functionalized Pd^{II} photoredox catalyst for Sonogashira C-C cross-coupling reactions, Chem. Commun. 55 (2019) 4973–4976.
[11] Y.B. Platonova, A.N. Volov, L.G. Tomilova, Palladium(II) octaalkoxy- and octaphenoxyphthalocyanines: synthesis and evaluation as catalysts in the Sonogashira reaction, J. Catal. 373 (2019) 222–227.
[12] M.B. Thathagar, J. Beckers, G. Rothenberg, Palladium-free and ligand-free Sonogashira cross-coupling, Green Chem. 6 (2004) 215–218.
[13] H. Plenio, Katalysatoren für die Sonogashira-Kupplung-unedle Metalle auf dem Vormarsch, Angew. Chem. Int. Ed. 120 (2008) 7060–7063.
[14] O. Vechorkin, D. Barmaze, V. Proust, X.L. Hu, Ni-catalyzed Sonogashira coupling of nonactivated alkyl halides: orthogonal functionalization of alkyl iodides, bromides, and chlorides, J. Am. Chem. Soc. 131 (2009) 12078–12079.
[15] Y.Y. Li, X. Feng, Z.H. Li, Visible-light-initiated Sonogashira coupling reactions over CuO/TiO_2 nanocomposites, Catal. Sci. Technol. 9 (2019) 377–383.
[16] M. Shanmugam, A. Sagadevan, V.P. Charpe, V.K.K. Pampana, K.C. Hwang, Cu_2O nanocrystals-catalyzed photoredox Sonogashira coupling of terminal alkynes and arylhalides enhanced by CO_2, ChemSusChem 13 (2020) 287–292.
[17] C. Glaser, Contribution to the chemistry of phenylacetylenes, Ber 2 (1869) 422–424.
[18] A. Lei, M. Srivastava, X. Zhang, Transmetalation of palladium enolate and its application in palladium-catalyzed homocoupling of alkynes: a room-temperature, highly efficient route to make diynes, J. Org. Chem. 67 (2002) 1969–1971.
[19] I.J.S. Fairlamb, P.S. Bauerlein, L.R. Marrison, J.M. Dickinson, Pd-catalysed cross coupling of terminal alkynes to diynes in the absence of a stoichiometric additive, Chem. Commun. 34 (2003) 632–633.
[20] F. Alonso, M. Yus, Heterogeneous catalytic homocoupling of terminal alkynes, ACS Catal. 2 (2012) 1441–1451.
[21] P. Siemsen, R.C. Livingston, F. Diederich, Acetylenic coupling: a powerful tool in molecular construction, Angew. Chem. Int. Ed. 39 (2000) 2632–2657.
[22] X.B. Ke, S. Sarina, J. Zhao, X.G. Zhang, J. Chang, H.Y. Zhu, Tuning the reduction power of supported gold nanoparticle photocatalysts for selective reductions by manipulating the wavelength of visible light irradiation, Chem. Commun. 48 (2012) 3509–3511.
[23] Y.H. Xiao, Y.M. Huang, S. Xue, J. Zhao, Light switching of amine oxidation products from oximes to imines: superior activity of plasmonic gold nanorods-loaded TiO_2(B) nanofibers under visible-near IR light, Appl. Catal. B Environ. 265 (2020), 118596.
[24] E. Peiris, S. Sarina, E.R. Waclawik, G.A. Ayoko, P.F. Han, J.F. Jia, H.Y. Zhu, Plasmonic switching of the reaction pathway: visible-light irradiation varies the reactant concentration at the solid-solution interface of a gold-cobalt catalyst, Angew. Chem. Int. Ed. 58 (2019) 12032–12036.
[25] D.F. Swearer, H.Q. Zhao, L.N. Zhou, C. Zhang, H. Robatjazi, J.M.P. Martirez, C. M. Krauter, S. Yazdi, M.J. McClain, E. Ringe, E.A. Carter, P. Nordlander, N.J. Halas, Heterometallic antenna reactor complexes for photocatalysis, Proc. Natl. Acad. Sci. USA 113 (2016) 8916–8920.
[26] J. Quiroz, E.C.M. Barbosa, T.P. Araujo, J.L. Fiorio, Y.C. Wang, Y.C. Zou, T. Mou, T. V. Alves, D.C. de Oliveira, B. Wang, S.J. Haigh, L.M. Rossi, P.H.C. Camargo, Controlling reaction selectivity over hybrid plasmonic nanocatalysts, Nano Lett. 18 (2018) 7289–7297.
[27] X. Qiu, M. Miyauchi, K. Sunada, M. Minoshima, M. Liu, Y. Lu, D. Li, Y. Shimodaira, Y. Hosogi, Y. Kuroda, K. Hashimoto, Hybrid Cu_xO/TiO_2 nanocomposites as risk-reduction materials in indoor environments, ACS Nano 6 (2012) 1609–1618.
[28] J. Zhao, Z. Zheng, S. Bottle, A. Chou, S. Sarina, H.Y. Zhu, Highly efficient and selective photocatalytic hydroamination of alkynes by supported gold nanoparticles using visible light at ambient temperature, Chem. Commun. 49 (2013) 2676–2678.
[29] S. Yu, P.K. Jain, The chemical potential of plasmonic excitations, Angew. Chem. Int. Ed. 132 (2020) 2101–2104.
[30] P. Christopher, H.L. Xin, A. Marimuthu, S. Linic, Singular characteristics and unique chemical bond activation mechanisms of photocatalytic reactions on plasmonic nanostructures, Nat. Mater. 11 (2012) 1044–1050.
[31] H.Y. Jiang, P. Zhou, Y. Wang, R. Duan, C. Chen, W. Song, J. Zhao, Copper-based coordination polymer nanostructure for visible light photocatalysis, Adv. Mater. 28 (2016) 9776–9781.
[32] A. Sagadevan, A. Ragupathi, K.C. Hwang, Photoinduced copper-catalyzed regioselective synthesis of indoles: three-component coupling of arylamines, terminal alkynes, and quinones, Angew. Chem. Int. Ed. 54 (2015) 13896–13901.
[33] P. Xiao, C.X. Li, W.H. Fang, G. Cui, W. Thiel, Mechanism of the visible-light-mediated copper-catalyzed coupling reaction of phenols and alkynes, J. Am. Chem. Soc. 140 (2018) 15099–15113.
[34] J. Bushell, A.F. Carley, M. Coughlin, P.R. Davies, D. Edwards, D.J. Morgan, M. Parsons, The reactive chemisorption of alkyl iodides at Cu(110) and Ag(111) surfaces: a combined STM and XPS study, J. Phys. Chem. B 109 (2005) 9556–9566.
[35] D. Syomin, B.E. Koel, Adsorption of iodobenzene (C_6H_5I) on Au(111) surfaces and production of biphenyl (C_6H_5-C_6H_5), Surf. Sci. 490 (2001) 265–273.
[36] P. Venkatesan, J. Santhanalakshmi, Synthesis of gold-palladium bimetallic nanoparticles and surface catalytic activity in suzuki coupling reactions using in FTIR spectroscopy, Am. J. Mater. Sci. 2 (2012) 82–86.
[37] C. Le, T.Q. Chen, T. Liang, P. Zhang, D.W.C. MacMillan, A radical approach to the copper oxidative addition problem: trifluoromethylation of bromoarenes, Science 360 (2018) 1010–1014.
[38] Y.N. Li, J.L. Wang, L.N. He, Copper(II) chloride-catalyzed glaser oxidative coupling reaction in polyethylene glycol, Tetrahedron Lett. 52 (2011) 3485–3488.
[39] A.E. Wendlandt, A.M. Suess, S.S. Stahl, Copper-catalyzed aerobic oxidative C-H functionalizations: trends and mechanistic insights, Angew. Chem. Int. Ed. 50 (2011) 11062–11087.
[40] R. Bai, G. Zhang, H. Yi, Z. Huang, X. Qi, C. Liu, J.T. Miller, A.J. Kropf, E.E. Bunel, Y. Lan, A. Lei, Cu(II)-Cu(I) synergistic cooperation to lead the alkyne C-H activation, J. Am. Chem. Soc. 136 (2014) 16760–16763.
[41] B. Wang, X.N. Guo, G.Q. Jin, X.Y. Guo, Visible-light-enhanced photocatalytic Sonogashira reaction over silicon carbide supported Pd nanoparticles, Catal. Commun. 98 (2017) 81–84.